

Analytical and Finite Element Solutions for Bending of Functionally Graded Piezoelectric Beams

A. Komeili¹, A. Armin², M. Abbasi³ and M.R. Eslami⁴

¹ M.Sc. Student, Amirkabir University of Technology, Tehran, Iran; komeili.amin@gmail.com

² M.Sc. Student, Amirkabir University of Technology, Tehran, Iran; ahad_armin_mec84@yahoo.com

³ Research Assistant, Amirkabir University of Technology, Tehran, Iran; musan.abbasi@gmail.com

⁴ Professor, Amirkabir University of Technology, Tehran, Iran; eslami@aut.ac.ir

Abstract

This paper makes attempt to investigate bending of functionally graded piezoelectric beams based on the Euler-Bernoulli beam theory under mechanical loads. The beam with functionally graded piezoelectric material (FGPM) is graded in the thickness direction and a power law distributes the piezoelectric material properties. The electric potential is assumed linear across the beam thickness. The governing equations are obtained using the potential energy and the Hamilton's principle. The analytical solution of simply supported functionally graded piezoelectric beam is obtained by the finite Fourier transformation. Finite element results presented in this paper are compared with analytical solutions.

Keywords: functionally graded piezoelectric material; beam; static analysis; analytical solution; finite element

Introduction

Piezoelectric actuators and sensors have novel applications for microelectromechanical systems and smart material systems, especially in the medical and aerospace industries. Since most aerospace applications involve operations in changing thermal environments, increased interests in piezothermoelasticity during recent years have addressed thermo-and electromechanical responses [1]. For a piezoelectric laminate with homogeneous material properties in layers, large bending displacements, high stress concentrations and failure from interfacial rebinding are usually presented at the layer interfaces under mechanical or electric loading which may lead to lifetime limitations and reliability reduction. To reduce the drawbacks, piezoelectric materials and structures with functionally graded material properties along layer-thickness direction have been introduced and fabricated [2]. Smart structures or elements made of these so-called FGPMs are usually superior to the conventional sensors and actuators are often made of the uni-morph, the bi-morph and the multimorph materials. In the present study, bending analysis of functionally graded piezoelectric beam has been carried out under mechanical load by using the finite Fourier transformation and finite element method.

Derivation of the Governing Equations

Consider a functionally graded piezoelectric beam as shown in Figure 1. The material properties change functionally between the upper and lower surfaces

across the beam thickness. In the model that used in this paper, the material properties are expressed as

$$P(z) = P_{ul} \left(\frac{2z+h}{2h} \right)^n + P_l \quad P_{ul} = P_u - P_l \quad (1)$$



Figure 1: The FGPM beam and coordinates

Where z is coordinate in the thickness direction of a beam, (P_u, P_l) are the properties of the upper surface and the lower surface, respectively; and h is the thickness of the FGPM beam. Power n is the volume fraction exponent.

Using the Euler-Bernoulli theory, the displacement components are

$$u(x, z) = u_0(x) - zw_{,x}, \quad w(x) = w_0(x). \quad (2)$$

Where u is the axial displacement, w is the transverse displacement in the z direction. The subscript zero denotes middle surface displacement and the normal strain is given by

$$\varepsilon_x = \frac{\partial u_0}{\partial x} - z \frac{\partial^2 w_0}{\partial x^2} \quad (3)$$

The constitutive relationships describing the electrical and mechanical interactions for piezoelectric materials are given as

$$\begin{aligned} \sigma_{ij} &= c_{ijkl} \varepsilon_{kl} - e_{ij} E_l \\ D_i &= e_{ikl} \varepsilon_{kl} + \eta_{il} E_l \end{aligned} \quad (4)$$

Here, σ_{ij} and ε_{kl} are the stress and strain tensors respectively, D_i is the electrical displacement vector, $E_l = -\varphi_{,l}$ is the electrical field vector and φ is the electrical potential, c_{ijkl} is the elasticity matrix, e_{ikl} is the piezoelectric constant matrix, η_{il} is the dielectric permittivity coefficient matrix.

The general three-dimensional linear constitutive equations for the stresses and the electric displacements based on the Euler-Bernoulli theory reduce to

$$\begin{aligned}\sigma_x &= \hat{E}(z)(u_{0,x} - zw_{,xx}) + e_{31}(z)\varphi_{,z}, \\ D_z &= e_{31}(z)(u_{0,x} - zw_{,xx}) - \eta_{33}(z)\varphi_{,z}.\end{aligned}\quad (5)$$

Where, \hat{E} is Young's modulus. For mathematical simplification, the potential φ is assumed linear across the FGPM beam thickness as [3]

$$\varphi(x, z) = \frac{z}{h}(\varphi^+(x) - \varphi^-(x)) + \frac{1}{2}(\varphi^+(x) + \varphi^-(x)). \quad (6)$$

Where, φ^+ and φ^- are the electric potentials on the upper and lower surfaces of the FGPM beam, respectively. For static analysis of the beam, the virtual work done by the electromechanical internal forces in the FGPM beam is

$$\delta H = \int_V (\sigma_x \delta \varepsilon_x - D_z \delta E_z) dv. \quad (7)$$

Using Eqs. 5 and the electric field relations of Eq. 6, and substituting into Eq. 7 and using virtual work by carrying the variational formulation, the governing equations are obtained as

$$\begin{aligned}\delta u_0 : A'_1 u_{0,xx} + A'_2 \psi_{,xxx} + A'_3 \varphi_{,x}^+ + A'_4 \varphi_{,x}^- &= 0, \\ \delta w_0 : B'_1 u_{0,xxx} + B'_2 w_{0,xxx} + B'_3 \varphi_{,xx}^+ + B'_4 \varphi_{,xx}^- &= B'_5, \\ \delta \varphi^+ : C'_1 u_{0,x} + C'_2 w_{0,xx} + C'_3 \varphi^+ + C'_4 \varphi^- &= 0, \\ \delta \varphi^- : D'_1 u_{0,x} + D'_2 w_{0,xx} + D'_3 \varphi^+ + D'_4 \varphi^- &= 0,\end{aligned}\quad (8)$$

Where A' , B' , C' , D' , and E' are given in Appendix A.

Solution Procedure Based on Finite Fourier

To solve the simultaneous governing equations, dimensionless values are defined as

$$\bar{u}_0 = \frac{u}{l}, \quad \bar{x} = \frac{x}{l}, \quad \bar{w}_0 = \frac{w_0}{l}, \quad \bar{\varphi}^+ = \frac{e_{31u}}{\hat{E}_u l} \varphi^+, \quad \bar{\varphi}^- = \frac{e_{31u}}{\hat{E}_u l} \varphi^-. \quad (9)$$

Where l is the length of the beam, \hat{E}_u and e_{31u} are the Young's modulus and piezoelectric constant of the upper surface of the FGPM beam, respectively. The sign (-) indicates dimensionless value.

Using the dimensionless parameters, the governing Eqs.(8) are given as

$$\begin{aligned}a'_1 \bar{u}_{0,\bar{x}\bar{x}} + a'_2 \bar{w}_{0,\bar{x}\bar{x}\bar{x}} + a'_3 \bar{\varphi}_{,\bar{x}}^+ + a'_4 \bar{\varphi}_{,\bar{x}}^- &= 0, \\ b'_1 \bar{u}_{0,\bar{x}\bar{x}\bar{x}} + b'_2 \bar{w}_{0,\bar{x}\bar{x}\bar{x}} + b'_3 \bar{\varphi}_{,\bar{x}\bar{x}}^+ + b'_4 \bar{\varphi}_{,\bar{x}\bar{x}}^- &= b'_5, \\ c'_1 \bar{u}_{0,\bar{x}} + c'_2 \bar{w}_{0,\bar{x}\bar{x}} + c'_3 \bar{\varphi}^+ + c'_4 \bar{\varphi}^- &= 0, \\ d'_1 \bar{u}_{0,\bar{x}} + d'_2 \bar{w}_{0,\bar{x}\bar{x}} + d'_3 \bar{\varphi}^+ + d'_4 \bar{\varphi}^- &= 0.\end{aligned}\quad (10)$$

Where a'_1, b'_1, c'_1, d'_1 and b'_5 are dimensionless constants. In the present analysis, an analytical solution is obtained for the simply supported FGPM beams with the following boundary conditions as

$$\begin{aligned}\sigma_x = 0 &\quad \rightarrow \bar{u}_{,\bar{x}} = 0 &\quad \bar{x} = 0, 1, \\ \bar{w} = 0 & &\quad \bar{x} = 0, 1, \\ \bar{\varphi} = 0 &\quad \rightarrow \bar{\varphi}^+ = \bar{\varphi}^- = 0 &\quad \bar{x} = 0, 1.\end{aligned}\quad (11)$$

According to boundary conditions, to solve the system of equations Eqs.(7) a finite Fourier transformation can be used as

$$\begin{aligned}\bar{u}_{0m} &= \int_0^1 \bar{u}_0(\bar{x}) \cos(m\pi\bar{x}) d\bar{x}, \\ \bar{w}_m &= \int_0^1 \bar{w}(\bar{x}) \sin(m\pi\bar{x}) d\bar{x}, \\ \bar{\varphi}_m^+ &= \int_0^1 \bar{\varphi}_m^+(\bar{x}) \sin(m\pi\bar{x}) d\bar{x}, \\ \bar{\varphi}_m^- &= \int_0^1 \bar{\varphi}_m^-(\bar{x}) \sin(m\pi\bar{x}) d\bar{x}.\end{aligned}\quad (12)$$

Formulas for the inverse of transformation are obtained by using relationship from the theory of Fourier series. To obtain the m th Fourier components of unknown variables, the system of equations Eqs.(7) must be solved based on the choice of m . Also finite element model is developed and FEM results are compared with analytical solution.

Solution Procedure Based on Finite Element Method

Displacements and strains

The formulation presented here is based on Euler-Bernoulli beam theory, which leads to the following displacement field:

$$\{\bar{u}\} = \begin{Bmatrix} u \\ w \end{Bmatrix} = \begin{Bmatrix} u_0 \\ w_0 \end{Bmatrix} - \begin{Bmatrix} z \frac{\partial w_0}{\partial x} \\ 0 \end{Bmatrix} = [H][\bar{u}] \quad (13)$$

Where $\{\bar{u}\} = \{u_0, w_0, \partial w / \partial x\}^T$ are the midplane displacements in the x and z directions, and the rotation of the xz planes due to bending, and

$$H = \begin{bmatrix} 1 & 0 & -z \\ 0 & 1 & 0 \end{bmatrix} \quad (14)$$

Variational formulation

The potential energy H stored in a lamina comprises the various components of the elastic strain energy, piezoelectric energy and electrical energy; this is given by [4]

$$\begin{aligned}H(\varepsilon, E) &= \frac{1}{2} c_{ijkl} \varepsilon_{ij} \varepsilon_{kl} - e_{kji} E_i \varepsilon_{kl} \\ &\quad - \frac{1}{2} \eta_{ij} E_i E_j\end{aligned}\quad (15)$$

The constitutive Eqs. (4) are related to the potential energy by

$$\sigma_{ij} = \frac{\partial H}{\partial \varepsilon_{ij}} \quad D_i = -\frac{\partial H}{\partial E_i}. \quad (16)$$

Thus, from using Hamilton's principle, the variational form of the equations of motion for the beam can be written as

$$\begin{aligned}
& \delta \int_{t_0}^{t_1} \int_V \left[\frac{1}{2} \rho \dot{u}_i \dot{u}_i - H(\varepsilon_{ij}, E_i) \right] dv dt \\
& + \int_{t_0}^{t_1} \int_V f_{bi} \delta u_i dv dt + \int_{t_0}^{t_1} \int_S f_{ci} \delta u_i ds \\
& + \int_{t_0}^{t_1} \int_S (f_{si} \delta u_i + q \delta \varphi) ds dt = 0
\end{aligned} \quad (17)$$

Or

$$\begin{aligned}
& \delta \int_{t_0}^{t_1} \int_V (\rho \ddot{u}_i \delta u_i + \sigma_{ij} \delta \varepsilon_{ij} - D_i \delta E_i) dv dt \\
& + \int_{t_0}^{t_1} \int_V f_{bi} \delta u_i dv dt + \int_{t_0}^{t_1} \int_S f_{ci} \delta u_i ds \\
& + \int_{t_0}^{t_1} \int_S (f_{si} \delta u_i + q \delta \varphi) ds dt = 0
\end{aligned} \quad (18)$$

Here, t_0 and t_1 describe two arbitrary time values, δ is the variational operator, V and S denote the volume and surface of the solid, respectively. ρ is the density of the beam, q is the electrical surface charge, f_{bi} , f_{ci} and f_{si} represent the body forces, concentrated load and specified traction, respectively.

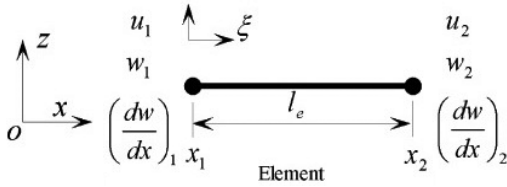


Figure 2: Two-node beam element and local coordinates system.

Finite element model

The analytical formulation described above is complete and solutions can be obtained from it. An exact solution may be adopted to solve a special problem or a finite element approach may be used to solve a more general problem. For the finite element formulation, the degrees of freedom consist of the mechanical variables and electric potential. At this point, the finite element will use a two-nodes Hermitian beam element [5]. The aim of the following derivations is to declare the strain-displacement, electric potential relations using nodal values and shape functions and then to use this in the integrand of the generalized virtual work formulation.

Hermitian beam element

The mechanical variable Eq. (13) that is based on the displacement of Euler-Bernoulli theory will be converted to its finite element representation using appropriate shape functions and mechanical nodal variables. The mechanical element being regarded is a 1D Hermitian beam element for transverse displacements, as shown in Figure 2. The two mechanical variables $\{u\}$ will be expressed using three mechanical nodal variables $\{u^e\}$ as follows:

$$\{u\} = [H][N]\{u^e\} \quad (19)$$

Where

$$\{u^e\} = \{u_1, w_1, (dw/dx)_1, u_2, w_2, (dw/dx)_2\}^T,$$

shape function matrix

$$N = \begin{bmatrix} \psi_1 & 0 & 0 & \psi_2 & 0 & 0 \\ 0 & g_{11} & g_{12} & 0 & g_{22} & g_{21} \\ 0 & \frac{\partial g_{11}}{\partial x} & \frac{\partial g_{12}}{\partial x} & 0 & \frac{\partial g_{22}}{\partial x} & \frac{\partial g_{21}}{\partial x} \end{bmatrix} \quad (20)$$

In which ψ is the Lagrangian shape function defined as: [5]

$$\begin{cases} \psi_1 \\ \psi_2 \end{cases} = \frac{1}{2} \begin{cases} 1-\zeta \\ 1+\zeta \end{cases} \quad (21)$$

And g_{ij} is the non-conforming Hermit cubic shape function can be expressed by

$$\begin{aligned}
g_{11} &= 1 - 3\left(\frac{1+\zeta}{2}\right)^2 + 2\left(\frac{1+\zeta}{2}\right)^3 & g_{22} &= \frac{1}{4}(1+\zeta)(2+\zeta-\zeta^2) \\
g_{12} &= \frac{1}{4}(1+\zeta)(1-\zeta)^2 & g_{21} &= \frac{1}{4}(1-\zeta)(1+\zeta)^2
\end{aligned} \quad (22)$$

Where ζ the local is coordinate defined as

$$\zeta = \frac{x - x_c}{a}, \quad -1 \leq \zeta \leq 1 \quad (23)$$

Using Eq. (19) and (3), the strain can be expressed as follows:

$$\varepsilon_x = [B_u]\{u^e\} \quad (24)$$

where $[B_u] = [L][N_u]$ is the strain interpolation matrix, and

$$[L] = \left[\frac{d}{dx}, 0, -z \frac{d}{dx} \right], \quad (25)$$

$$[B_u] = \left[\frac{\partial \psi_1}{\partial x}, -z \frac{\partial^2 g_{11}}{\partial x^2}, -z \frac{\partial^2 g_{12}}{\partial x^2}, \frac{\partial \psi_2}{\partial x}, -z \frac{\partial^2 g_{22}}{\partial x^2}, -z \frac{\partial^2 g_{21}}{\partial x^2} \right]$$

Again, using linear Lagrangian interpolation functions, the potential and electric field vector E can be defined in terms of nodal variables as

$$\varphi = [N_\varphi][\varphi^e] \quad (26)$$

$$E = -\nabla \varphi = -[B_\varphi]\{\varphi^e\} \quad (27)$$

$$[B_\varphi] = \nabla [N_\varphi] \quad (28)$$

Elementary governing equations of motion

The elementary governing equations of motion in general form can be derived by substituting Eqs. (16), (21) and (24) into Eq. (15) and assembling the element equations, which can be written as follows:

$$[M_{uu}]\{\ddot{u}\} + [K_{uu}]\{u\} + [K_{u\phi}]\{\phi\} = \{F_m\} \quad (29)$$

$$[K_{\phi u}]\{u\} - [K_{\phi\phi}]\{\phi\} = \{f_q\} \quad (30)$$

The respective matrices and vectors are given by

$$[M_{uu}] = \int_v [N]^T [H]^T [\rho] [H] [N] dv \quad (31)$$

$$[K_{uu}] = \int_v [B_u]^T [C] [B_u] dv \quad (32)$$

$$[K_{u\phi}] = \int_v [B_u] [e]^T [B_\phi] dv \quad (33)$$

$$[K_{\phi\phi}] = \int_v [B_\phi]^T [K] [B_\phi] dv \quad (34)$$

$$[F_q^e] = \int_{sq} [N]^T [q] ds \quad (35)$$

$$[F_m] = \int_v [N]^T [H]^T \{f_b\} dv + \int_{sf} [N]^T [H]^T \{f_s\} ds \quad (36)$$

where $[M_{uu}]$ is the mass matrix; $[K_{uu}]$ mechanical stiffness matrix; $[K_{u\phi}]$ the piezoelectric coupling matrices; $[K_{\phi\phi}]$ the dielectric primitivity matrix. $\{F_m\}$ and $\{F_q\}$ are the mechanical excitation and electric excitation vectors. Here it should be noted that the material properties are position-dependent. Substituting Eq. (30) into Eq. (29), we obtain

$$[M_{uu}]\{\ddot{u}\} + \left([K_{uu}] + [K_{u\phi}][K_{\phi\phi}]^{-1}[K_{\phi u}] \right) \{u\} = \{F_m\} + \left([K_{u\phi}][K_{\phi\phi}]^{-1} \right) \{F_q\} \quad (37)$$

For the static analysis problems, $\{\ddot{u}\} = 0$ the governing equations of motion in Eq. (34) reduces to

$$\left([K_{uu}] + [K_{u\phi}][K_{\phi\phi}]^{-1}[K_{\phi u}] \right) \{u\} = \{F_m\} + \left([K_{u\phi}][K_{\phi\phi}]^{-1} \right) \{F_q\} \quad (38)$$

Results and Discussion

A simply supported FGPM beam with the slenderness ratio ($l/h = 6$) and $l=0.025$ m subjected to uniform pressure $q = 10\text{kNm}^{-2}$ on top surface is considered for the study. The bottom surface of the FGPM beam is PZT-5H whereas the top surface of the beam is PZT-4A. The influence of material is examined by varying the power law exponent. The material properties of PZT-4 and PZT-5H are shown in Table 1.

Table 1. Material properties.

	PZT-4	PZT-5H
E (GPa)	74.1	55
K (W/m^0K)	75	75
e_{31} (C/m^2)	-5.2	-6.5
η_{33} (N/m^2)	1.15×10^{-8}	3×10^{-8}

Figure 2 depicts the distribution of the volume fraction along the thickness for different power law indices n . The dimensionless deflection through the dimensionless beam length is shown in Figure 3 for various volumes fraction exponent n that we compare the result of figure 3(a) and 3(b) in Table (2) to show the accuracy of results. It is seen that for larger values of n , the midpoint deflections of the FGPM beam is changed and increased evidently. Figure 4 shows the comparison of axial Stress of FGPM beam σ_x across the dimensionless height of beam between two solution of Finite Element and Finite Fourier. Also, Figure 5 shows the electric displacements D_z across the thickness direction of the FGPM beam caused by mechanical load for finite Fourier transformation and finite element model. It is seen that with increase of the power law index n in the range 0 to 2, $0 \leq n \leq 2$, the electric field of the FGPM beam is increased. For $n > 2$ the electric field start to decrease when n is increased to higher values because of difference range of two coefficients e_{31} , η_{33} in two materials PZT-4 and PZT-5H.

Conclusions

In the present paper, the effect of mechanical loads on the static behavior of a functionally graded piezoelectric beam using the Euler-Bernoulli beam theory has been investigated. The solution of governing equations is obtained using virtual work. Results are obtained by finite Fourier transformation and finite element model. Results show the displacements and stresses changes significantly and gradually for different power law indexes. Moreover, it can be said that finite element solutions converge very well to produce results in good agreement with the Finite Fourier transformation. This study suggests that it may be possible to choose an appropriate FGM profile for desired applications.

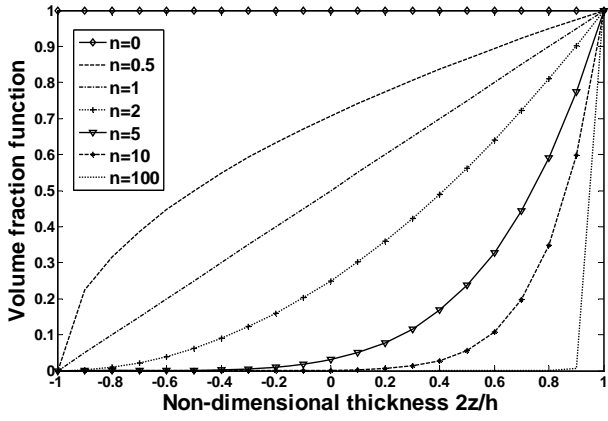
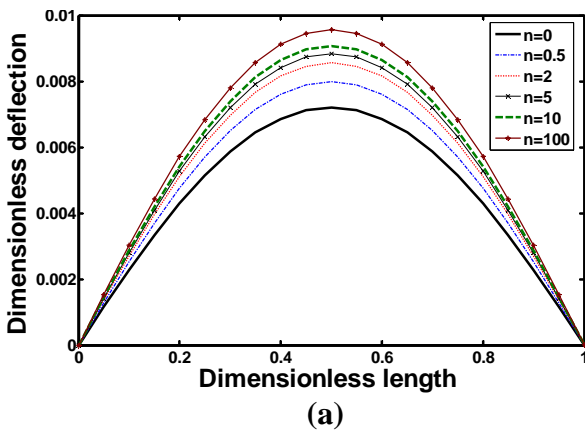


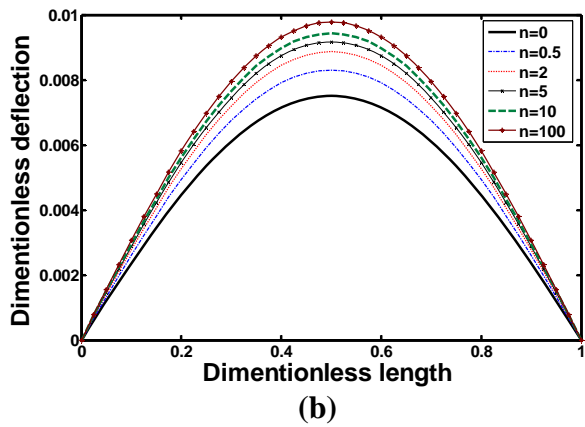
Figure 2. The distribution of the volume fraction along the thickness for different values of the power law indices, n .

Table 2. Comparison of Distribution of dimensionless deflection through the dimensionless length by Finite fourie transformation and Finite elemet method

n	Finite Fourier	Finite Element	Error%
0	0.007402	0.007504	1.37
0.5	0.008284	0.008307	0.27
2	0.008762	0.008865	1.17
5	0.009338	0.009428	0.95
10	0.009371	0.009428	0.61
100	0.009669	0.009780	1.15



(a)



(b)

Figure 3: Distribution of dimensionless deflection through the dimensionless length (a) Finite fourie transformation (b) Finite elemet method

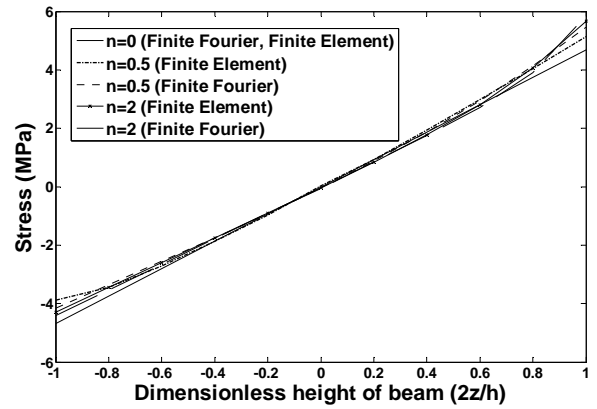


Figure4. Comparison of Distribution of Stress through the dimensionless height by Finite fourie transformation and Finite elemet method

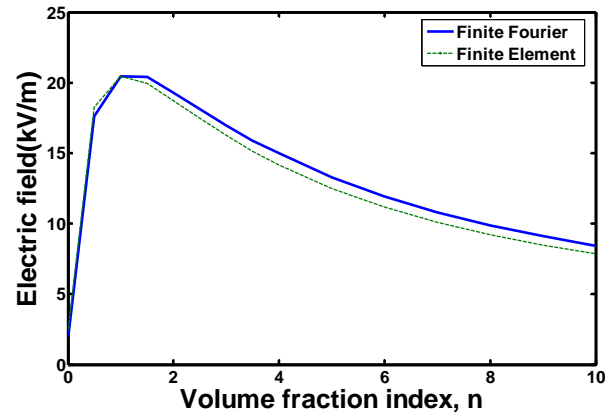


Figure5: Electric field versus volme fraction indexes for simply supported FGPM beam under mechanical load

References

- [1] H.J.Xiang., Z.F.Shi., 2008. Static analysis for multi-layered piezoelectric cantilevers. *International Journal of Solids and Structures* 45 (2008) 113–128
- [2] Shi, Z.F., Chen, Y., 2004. Functionally graded piezoelectric cantilever beam under load. *Archive of Applied Mechanics* 74, 237–247
- [3] Kapuria, S., Ahmed, A., Dumir, P.C., 2004. Coupled consistent third-order theory for hybrid piezoelectric beams under thermal load. *Journal of Thermal Stresses* 27,405-424.
- [4] K.M. Liew, S. Sivashanker, X.Q. He, and T.Y. Ng, The modeling and design of smart structures using functionally graded materials and piezoelectrical sensor/actuator, *Smart Mater. Struct.*, vol. 12, pp. 647-655, 2003.
- [5] J. P. Jiang, and D. X. Li, A new finite element model for piezothermoelastic composite beam, *J. Sound Vibr.*, vol. 306, pp. 849-864, 2007.
- [6] Lanhe, W., Hongjun, W. and Daobin W., 2007, "Nonlinear Dynamic stability analysis of FGM plates by the moving least squares differential quadrature method ", *Composite Structures*, **77**, 383-394.
- [7] Pin, L., Lee, H.P. and Lu, C., 2006, "Exact solutions for simply supported functionally graded piezoelectric laminates by Stroh-like formalism", *Composite Structures*, **72**, 352-363.
- [8] Wang, B.L., and Noda, N., 2001, "Design of a smart functionally graded Thermo piezoelectric composite structure ", *Smart Materials and Structures*, **10**, 189-193.
- [9] Liew, K.M., Sivashanker, S., He, X.Q., Ng, T.Y., 2003, "The modeling and design of smart structures using functionally graded materials and piezoelectrical sensor/actuator ", *Smart Materials and Structures*, **12**, 647-655.
- [10] Trindade, M.A .and Benjeddou, A., 2006, " On higher-order modeling of smart beams with embedded shear-mode piezoceramic actuators and sensors ", *Mechanics of Advanced Materials and Structures*, **13(5)**, 357-369.
- [11] Jin, D.R., Meng, Z.Y., 2003. "Functionally graded PZT/ZnO piezoelectric composites ", *J. Material Science Letters*, **22**, 971-974.

Appendix A

$$A'_1 = \int \hat{E}(z) dz,$$

$$A'_2 = \int -z\hat{E}(z) dz,$$

$$A'_3 = \int \frac{e_{31}(z)}{h} dz,$$

$$B'_1 = \int z\hat{E}(z) dz,$$

$$B'_2 = \int z^2\hat{E}(z) dz,$$

$$B'_3 = \int \left(\frac{ze_{31}(z)}{h} \right) dz,$$

$$B'_4 = \int_0^1 f_3 \sin(m\pi\bar{x}) d\bar{x},$$

$$C'_1 = \int e_{31}(z) dz,$$

$$C'_2 = -\int ze_{31}(z) dz,$$

$$C'_3 = \int -\frac{\eta_{33}(z)}{h} dz.$$